EAI Endorsed Transactions on
Industrial Networks and Intelligent Systems
EAI.EU Research Article

Optimizing Energy Harvesting Efficiency for IRS-aided TS-SWIPT System with Continuous and Discrete Phase Shifts

Pham Viet Tuan[1,*], Van-Quang-Binh Ngo[1], Quang Vinh Do[2], Insoo Koo[3]

[1]Faculty of Physics, University of Education, Hue University, Hue City, Vietnam
[2]Wireless Communications Research Group, Faculty of Electrical and Electronics Engineering, Ton Duc Thang University, Ho Chi Minh City, Vietnam
[3]Department of Electrical, Electronics and Computer Engineering, University of Ulsan, Ulsan 44610, South Korea

Abstract

In recent years, intelligent reflecting surfaces (IRS) have emerged as a groundbreaking technology for enhancing spectral and energy efficiency in wireless communication, offering a cost-effective and energy-efficient solution. This study explores a simultaneous wireless information and power transfer (SWIPT) network employing time-switching (TS) receivers, where a base station (BS) transmits both data and energy signals to users with the assistance of an IRS. By appropriately tuning the phase shifts of IRS elements, transmission performance is optimized in terms of both energy harvesting and data throughput efficiency. The primary objective is to maximize energy harvesting efficiency, defined as the ratio of total harvested energy at the users to the transmission power of the BS, while ensuring the required information rate, adhering to power constraints, and considering practical constraints on phase shifts. To tackle this challenge, iterative algorithms based on alternating optimization, non-convex approximations, feasible point pursuit is developed to jointly optimize information beamformers, energy covariance matrix, IRS phase shifts, and TS factors. Numerical simulations validate the convergence and effectiveness of the proposed method.

Received on 19 May 2025; accepted on 30 August 2025; published on 02 September 2025

Keywords: Energy harvesting e ciency, intelligent reflecting surface (IRS), SWIPT, time-switching (TS), continuous/ discrete phase shifts.

doi:10.4108/eetinis.v12i3.9356

1. Introduction

Recently, the rapid advancement of the Internet of Things (IoT) and machine-type communication (MTC) has shifted wireless networks toward large-scale machine and device connectivity, paving the way for the next stage of IoT in sixth-generation (6G) networks - known as the Internet of Everything (IoE) [1, 2]. The IoE is expected to support an exceptionally high connection density, reaching at least 10^7 devices per square kilometer, many of which will have limited power storage [3]. This widespread deployment of battery-constrained IoT devices presents a significant challenge, as frequent charging or battery substitution can be complex and costly, especially in applications such as body sensors. Conventional energy harvesting methods, including solar and wind power, have been explored to enhance self-sufficiency of energy-limited IoT devices. However, these techniques rely heavily on environmental conditions, making them unreliable in certain scenarios. To address this limitation, simultaneous wireless information and power transfer (SWIPT) has emerged as a viable alternative, leveraging wireless signals for energy harvesting [4–6].

*Corresponding author. Email: phamviettuan@dhsphue.edu.vn.
Emails: phamviettuan@dhsphue.edu.vn, pvtuan@hueuni.edu.vn (P.V. Tuan); ngovanquangbinh@dhsphue.edu.vn, nvqbinh@hueuni.edu.vn (V.Q.B. Ngo); dovinhquang@tdtu.edu.vn (Q.V. Do); iskoo@ulsan.ac.kr (I. Koo).
A part of this paper was presented in the International Conference on Industrial Networks and Intelligent Systems (INISCOM), 2024.

SWIPT receivers can be categorized into three main types based on how they distribute resources between energy harvesting and information decoding: time-switching (TS), power splitting (PS), and antenna switching (AS) [7]. The PS receiver increases system complexity, while the AS receiver requires multiple antennas. In contrast, the TS-based SWIPT architecture is a suitable option for low-power IoT devices, especially those with a single-antenna design [8–10]. Regarding TS strategies, the study in [11] simultaneously optimized TS parameters and transmit covariance matrices within a two-user SWIPT Multiple-Input Single-Output (MISO) framework to enhance the achievable rate region. Meanwhile, research in [12] addressed the energy efficiency (EE) optimization challenge for a TS-enabled Non-Orthogonal Multiple Access (NOMA) system by jointly designing TS coefficients and power allocation. In [13], the coexisting users with the PS/TS schemes are investigated to minimize the base station's transmission power.

The Intelligent Reflecting Surface (IRS), also known as the Reconfigurable Intelligent Surface (RIS), has recently emerged as a cutting-edge technology for modifying wireless signal propagation and enhancing network efficiency [14–17]. Consisting of an array of reflective elements, each capable of dynamically adjusting its phase, IRS empowers constructive signal reinforcement at target devices while mitigating interference through phase alignment. Notably, IRS operates passively, reflecting signals without amplification, thereby reducing hardware complexity and power consumption. Additionally, its thin and lightweight structure allows seamless integration onto surfaces such as walls and windows, enabling easy deployment without requiring modifications to existing network infrastructure. Given the significant potential of SWIPT and IRS in boosting EE, extensive research has explored their integration. One of the earliest studies [18] examined an IRS-assisted SWIPT system, optimizing the weighted sum power of energy-harvesting (EH) receivers.

In [19], the authors considered future self-sustainable Internet of Things (SS-IoT) network cooperating with another network via an IRS. The energy efficiency, defined as the ratio between the sum rate and energy consumption, is maximized via the alternating optimization (AO) and semidefinite relaxation (SDR) methods. The authors also proposed a low-complexity approach by using heuristic beamforming vectors and an iterative method with an element-wise block-coordinate descent technique for IRS optimization. In [20], the authors considered the max-min signal-to-interference-plusnoise ratio (SINR) problem of IRS-aided SWIPT system with the power-splitting (PS) users. The AO, SDR, and bisection methods are employed to find the BS transmit beamforming vector, PS factors, and IRS phase shifts. In [21], the simultaneously transmitting and reflecting reconfigurable intelligent surface (STAR-RIS) assisted SWIPT system is studied with the separation of information users and energy harvesting users. The multi-objective optimization problem (MOOP) of max-min information rate and max-min harvested power is formulated and solved by the AO, SDR, and bisection methods. In [22], the STAR-RIS assisted SWIPT system cooperating rate splitting multiple access (RSMA) technique is investigated. The balance of users' sum rate and total harvested power is optimized using a meta deep deterministic policy gradient (Meta-DDPG) method. In [23], the STAR-RIS enhanced SWIPT system is studied with the aim of maximizing weighted sum power as well as separating ID and EH users. The SDR and Gaussian randomization methods are applied under three RIS protocols: energy splitting (ES), mode splitting (MS), and time switching (TS). In [24], the authors studied STAR-RIS in autonomous aerial vehicle (AAV) networks with SWIPT serving multiple outdoor energy users and multiple indoor information users. The goal is to minimize the total AAV energy consumption subject to the required ID/EH thresholds for users and the AAV flight constraints. We observe that most work on STAR-RIS SWIPT focus on PS users or on separating ID/EH users (i.e., do not consider TS users) and target either total harvested energy or data-rate maximization. Additional studies have analyzed various benefits of IRS-enhanced SWIPT frameworks, addressing key challenges such as EE optimization [25, 26], maximizing the weighted sum rate [27], minimizing transmit power [28], and increasing total harvested energy [29].

This research aims to maximize energy harvesting efficiency, defined as the ratio of total energy collected by users to the transmission power of the base station (BS), in a TS-SWIPT network by utilizing the adjustable phase shifts of IRS reflective components. This objective ensures efficient energy utilization while simultaneously supporting reliable information transmission. Firstly, we remark that most prior works focused on PS receivers or on separating EH and ID receivers in IRS-aided SWIPT system [20, 29, 30]. Secondly, the highly non-convex target and constraint functions in the TS-SWIPT framework are fundamentally different from those studied in previous works. Moreover, while conventional optimization approaches such as successive convex approximation (SCA) and alternating optimization (AO) [31, 32] have been widely adopted in the literature, this work introduces novel formulations and proposes efficient solution algorithms with feasible point pursuit (FPP) method [33] and Taylor expansion to address the challenging EH efficiency maximization problem involving strongly non-convex functions,

thereby achieving the desired performance gains. Additionally, tthe IRS phase shifts are treated in both continuous and discrete forms. Our main contributions are described as follows.

1. In the proposed IRS-aided SWIPT system, a multi-antenna base station transmits both individual information streams and energy to multiple single-antenna receivers equipped with TS circuits. objective is to maximize EH efficiency by jointly optimizing BS transmission vector, energy transmission covariance matrix, TS coefficients, and continuous/discrete IRS phase shifters while guaranteeing the receivers' data rate requirements and BS transmit power constraint.
2. We first transform the complex EH efficiency maximization problem into a tractable form by introducing auxiliary variables. Then, the AO method is employed to decouple transceiver variables and IRS parameters. For each subproblem, the solution is obtained by combining mathematical transformation with the SCA and FPP techniques to handle the complicated non-convex constraints. To sum up, the effective algorithms are proposed to compute the suboptimal parameters for both continuous and discrete phase-shift cases.
3. Finally, numerical results demonstrate that the proposed iterative algorithms achieves rapid convergence and improve the EH efficiency with both continuous and discrete phases compared to the baseline without IRS. Moreover, incorporating IRS into the TS-SWIPT network enhances energy utilization across a wide range of system parameter settings.

The rest of this study is structured as follows. Section 2 describes the system model and formulates the optimization problem. Section 3 illustrates the proposed approach for maximizing EH efficiency. Section 4 presents numerical simulations that evaluate system performance, followed by concluding remarks in Section 5.

Notations: Bold lowercase letters represent vectors, while bold uppercase letters signify matrices. $\mathbb{E}(\cdot)$, $\mathrm{Re}(\cdot)$, $\mathrm{Tr}(\cdot)$, and $(\cdot)^H$ indicate the expectation, real part, trace and transpose-conjugate operations, respectively. $|u|$ and $\|\mathbf{u}\|$ denote the magnitude and Euclid norm of a complex scalar u and a complex vector $\mathbf{u}$, respectively. In addition, $\mathrm{diag}(\mathbf{u})$ denotes as a diagonal matrix with each diagonal element given by the corresponding component in $\mathbf{u}$. $\mathbb{C}^{k\times l}$ is denoted as the space of $k \times l$ complex matrices. A circularly symmetric complex Gaussian distribution with mean ζ and variance ϖ^2 is denoted as $\mathcal{CN} \sim \left(\zeta, \varpi^2\right)$. $\mathbf{B}_{k,l}$ indicates the element at the k-th row and the l-th column in matrix $\mathbf{B}$.

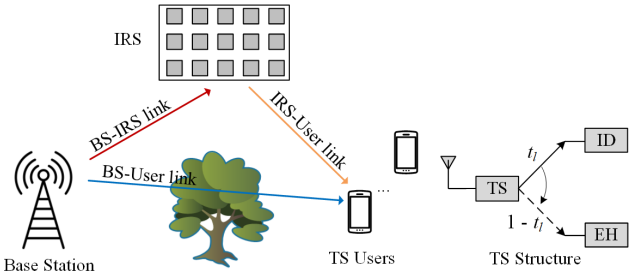

Figure 1. Description of the IRS-assisted TS-SWIPT network.

2. Network Description and Optimization Problem

In the section, the IRS-assisted SWIPT network with multiple TS users is presented and the EH efficiency maximization problem is expressed for optimizing system parameters. The major notations and meaning description are listed in Table 1.

Table 1. Major notations

Symbol	Description
M	BS antenna number
N	IRS component number
L	User number
$\mathbf{G} \in \mathbb{C}^{N\times M}$	BS-IRS channel
$\mathbf{f}_{d,l} \in \mathbb{C}^{M\times 1}$	BS-lth user channel
$\mathbf{f}_{r,l} \in \mathbb{C}^{N\times 1}$	IRS-lth user channel
$\mathbf{b}_l \in \mathbb{C}^{M\times 1}$	BS beamformer for symbol s_l
$\mathbf{v} \sim \mathcal{CN}(0, \mathbf{V})$	Energy transmission vector
$P_{T,\max}$	Maximum transmission power at BS
$\mathbf{\Phi}$	IRS phase shift matrix
t_l	Time duration for ID at l-th user
φ_n	Shifted phase at n-th component
γ_l	Target information rate at l-th user

2.1. Network Description

The SWIPT network under consideration consists of a single BS, an IRS, and multiple time-switching user devices, as illustrated in Fig. 1 [34]. The base station is equipped with multiple antennas for signal transmission, while each user device is equipped with a single antenna and a time-switching mechanism. The IRS comprises elements that are configured to enhance the incoming RF signals, thereby improving energy and data transfer. We denote the channels from the BS and IRS to the l-th device as $\{\mathbf{f}_{d,l}, \mathbf{f}_{r,l}\}$, $\forall l \in \{1, 2, \cdots, L\}$ where $\mathbf{f}_{d,l} \in \mathbb{C}^{M\times 1}$, $\mathbf{f}_{r,l} \in \mathbb{C}^{N\times 1}$. Moreover, the BS-IRS channel is denoted as $\mathbf{G} \in \mathbb{C}^{N\times M}$.

Our proposed solution is based on the assumption that perfect channel state information (CSI) is available at both the BS and the passive IRS. In practice, obtaining

accuracy CSI is challenging due to limitations of low-cost hardware that can only reflect signals. The considered low-cost IRS is purely passive without amplifying units, and with limited signal processing capability thus it cannot employ the pilot symbol transmission protocol as conventional active transceivers do. In [35], the cascaded BS-IRS and IRS-receiver channels were estimated and used for system design. However, due to the large number of IRS elements, exchanging channel coefficients leads to high channel estimation overhead for IRS utilization. The issues of CSI accuracy and feedback overhead reduction are studied in [36, 37]. The assumption of perfect CSI for BS-IRS and IRS-receiver channels in our work is consistent with prior works [20, 30]. The inevitable CSI uncertainties can be addressed by applying the worst-case robust for bounded CSI error model [21, 38] or by the stochastic optimization for statistical CSI error model [39, 40]. The S-procedure [41] and Bernstein-Type inequality [42] methods can be employed for these CSI error cases. These extensions will be studied in future works. We remark that the results in our work can serve as an upper bound under practical CSI uncertainties and provide a valuable solution for EH efficiency design in IRS-assisted TS-SWIPT systems. Moreover, in practice, implementation is difficult due to the high cost of designing high-resolution phase shifter controllers. Hence, IRS phase quantization is adopted to enable a more cost-efficient realization of IRSs, where discrete and finite phase-shift levels, requiring only a limited number of control bits are employed and presented in subsection 3.3.

The phase-shift matrix is defined as $\mathbf{\Phi} = \text{diag}\left(e^{j\varphi_1}, e^{j\varphi_2}, \cdots, e^{j\varphi_N}\right)$ for the IRS with imaginary unit j. Moreover, $\varphi_n \in [0, 2\pi)$, $\forall n \in \{1, 2, \cdots, N\}$, represents the shifted angles at the n-th IRS element. The BS' s transmission signal is formulated as $\mathbf{x}_B = \sum_{l=1}^{L} \mathbf{b}_l s_l + \mathbf{v}$, where the beamforming vector $\mathbf{b}_l \in \mathbb{C}^{M\times 1}$, is precoded for sending data symbol s_l to the l-th TS device. In addition, an energy transmission vector $\mathbf{v}$, represented as a Gaussian pseudo-random sequence, is employed for energy harvesting along with an associated covariance matrix $\mathbf{v} \sim \mathcal{CN}(0, \mathbf{V})$. Consequently, the signal reflected by the intelligent surface is represented as $\mathbf{x}_{IRS} = \mathbf{\Phi G}\left(\sum_{l=1}^{L} \mathbf{b}_l s_l + \mathbf{v}\right)$ and the signal obtained by the l-th time-switching user is expressed as

$$r_l = \left(\mathbf{f}_{r,l}^H \mathbf{\Phi G} + \mathbf{f}_{d,l}^H\right)\left(\sum_{l=1}^{L} \mathbf{b}_l s_l + \mathbf{v}\right) + n_l, \forall l \qquad (1)$$

where the Gaussian noise, $n_l \sim \mathcal{CN}\left(0, \sigma_l^2\right)$, is presented at the l-th user. Utilizing the TS framework, users can alternate between information decoding (ID) and EH modes to receive both power and data. Without loss of generality, assuming each operational period is normalized to a unit time, the respective time duration allocated for ID and EH at the l-th user are denoted as t_l and $(1 - t_l)$. Consequently, the amount of energy harvested from the incident signal at the l-th user is determined by

$$\Lambda_l = (1 - t_l)\left(\begin{array}{l} \sum_{k=1}^{L} \left|\left(\mathbf{f}_{d,l}^H + \mathbf{f}_{r,l}^H \mathbf{\Phi G}\right)\mathbf{b}_k\right|^2 \\ +\text{Tr}\left(\left(\mathbf{f}_{d,l}^H + \mathbf{f}_{r,l}^H \mathbf{\Phi G}\right)\left(\mathbf{f}_{d,l}^H + \mathbf{f}_{r,l}^H \mathbf{\Phi G}\right)^H \mathbf{V}\right) \end{array}\right) \qquad (2)$$

Additionally, the data transmission rate is obtained based on the signal-to-interference-plus-noise ratio (SINR) as

$$\Theta_l = t_l \log_2\left(1 + \frac{\left|\left(\mathbf{f}_{d,l}^H + \mathbf{f}_{r,l}^H \mathbf{\Phi G}\right)\mathbf{b}_l\right|^2}{\sum_{k\neq l}^{L} \left|\left(\mathbf{f}_{d,l}^H + \mathbf{f}_{r,l}^H \mathbf{\Phi G}\right)\mathbf{b}_k\right|^2 + \text{Tr}\left(\mathbf{F}_l \mathbf{V}\right) + \sigma_l^2}\right) \qquad (3)$$

2.2. Optimization Problem for Energy Harvesting Efficiency

The power emitted from the BS is represented as

$$\text{P}_B = \sum_{l=1}^{L} \|\mathbf{b}_l\|^2 + \text{Tr}\left(\mathbf{V}\right). \qquad (4)$$

The cumulative harvested energy across all users, based on the linear EH model, is calculated as

$$\sum_{l=1}^{L} \Lambda_l = \sum_{l=1}^{L}\left[(1 - t_l)\left(\sum_{k=1}^{L} \left|\left(\mathbf{f}_{d,l}^H + \mathbf{f}_{r,l}^H \mathbf{\Phi G}\right)\mathbf{b}_k\right|^2 + \text{Tr}\left(\mathbf{F}_l \mathbf{V}\right)\right)\right] \qquad (5)$$

with $\mathbf{F}_l = \left(\mathbf{f}_{d,l}^H + \mathbf{f}_{r,l}^H \mathbf{\Phi G}\right)^H \left(\mathbf{f}_{d,l}^H + \mathbf{f}_{r,l}^H \mathbf{\Phi G}\right)$. We set the EH efficiency as $f_{EHE}\left(\mathbf{b}_l, \mathbf{V}, t_l, \varphi_n\right) =$

$$\frac{\sum_{l=1}^{L}\left[(1 - t_l)\left(\sum_{k=1}^{L} \left|\left(\mathbf{f}_{d,l}^H + \mathbf{f}_{r,l}^H \mathbf{\Phi G}\right)\mathbf{b}_k\right|^2 + \text{Tr}\left(\mathbf{F}_l \mathbf{V}\right)\right)\right]}{\sum_{l=1}^{L} \|\mathbf{b}_l\|^2 + \text{Tr}\left(\mathbf{V}\right)} \qquad (6)$$

Then, the energy harvesting efficiency maximization problem is given by:

$$\underset{\{\mathbf{b}_l,\mathbf{V},t_l,\varphi_n\}}{\text{maximize}} \; f_{EHE}\left(\mathbf{b}_l,\mathbf{V},t_l,\varphi_n\right) \quad \text{subject to} \tag{7a}$$

$$t_l \log_2\left(1+\frac{\left|\left(\mathbf{f}_{d,l}^H+\mathbf{f}_{r,l}^H\mathbf{\Phi}\mathbf{G}\right)\mathbf{b}_l\right|^2}{\left(\begin{array}{l}\sum\limits_{k=1,k\neq l}^{L}\left|\left(\mathbf{f}_{d,l}^H+\mathbf{f}_{r,l}^H\mathbf{\Phi}\mathbf{G}\right)\mathbf{b}_k\right|^2\\ +\mathrm{Tr}\left(\mathbf{F}_l\mathbf{V}\right)+\sigma_l^2\end{array}\right)}\right)\geq\gamma_l,\forall l \tag{7b}$$

$$\sum_{l=1}^{L}\|\mathbf{b}_l\|^2+\mathrm{Tr}\left(\mathbf{V}\right)\leq P_{T,\max} \tag{7c}$$

$$1\geq t_l\geq 0,\ \forall l,\mathbf{V}\succeq 0 \tag{7d}$$

$$\left|\mathbf{\Phi}_{n,n}\right|=1,\ \forall n,\varphi_n\in[0,2\pi),\ \forall n \tag{7e}$$

The objective in (7a) is to optimize EH efficiency within the IRS-assisted TS-SWIPT framework. Constraint (7b) ensures the quality of service by maintaining a minimum required information rate, γ_l, for the l-th user. Constraint (7c) imposes a transmission power limitation, restricting it to a maximum threshold, $P_{T,\max}$. Constraint (7d) defines the limitations on the TS ratio, energy covariance matrix, and phase-shift matrix. The formulated problem (7) is highly non-convex due to the presence of non-convex functions in both the objective function and constraints. We observe that the coupled four types of variables including BS beamformers, energy covariance matrices, TS factors, and IRS phase shifts lead to the highly complicated objective and constraint functions in the EH efficiency optimization problem. Therefore, the AO method is applied to separate two variable groups - transceiver parameters and IRS parameters - into two optimization subproblems. Since the functions in each subproblem are non-convex, the SCA method with Taylor expansion is used to transform these non-convex functions into the convex approximations. Then, we can solve the series of convex subproblems effectively by using CVX tool [43]. To guarantee the convergence of the SCA, the starting point must be a feasible point of the original optimization problem. To address this requirement, the FPP method introduces nonnegative auxiliary variables in the inequality constraints and adds them to the objective function. This procedure ensures that any starting point becomes feasible, while the auxiliary variables converge to zero as the SCA iterations proceed. In the next section, the proposed solution procedure is presented in detail.

3. Proposed Approach for Optimizing EH Efficiency

3.1. Design for BS and Users Parameters with Fixed Reflecting Phase Shifts

The objective function in (7a) has a complex structure, making it challenging to solve directly. To address this, we apply specific transformations to reformulate the non-convex optimization problem into a more tractable form. Initially, an auxiliary set of variables $\{x_l, y\}$ is introduced, allowing the objective function to be rewritten as:

$$\underset{\{\mathbf{b}_l,\mathbf{V},t_l,x_l,y\}}{\text{maximize}} \; \frac{\sum\limits_{l=1}^{L}x_l^2}{y} \quad \text{subject to} \tag{8a}$$

$$(1-t_l)\left(\sum_{k=1}^{L}\left|\left(\mathbf{f}_{d,l}^H+\mathbf{f}_{r,l}^H\mathbf{\Phi}\mathbf{G}\right)\mathbf{b}_k\right|^2+\mathrm{Tr}\left(\mathbf{F}_l\mathbf{V}\right)\right)\geq x_l^2,\forall l \tag{8b}$$

$$\sum_{l=1}^{L}\|\mathbf{b}_l\|^2+\mathrm{Tr}\left(\mathbf{V}\right)\leq y,\forall l \tag{8c}$$

$$x_l\geq 0,y\geq 0,\forall l \tag{8d}$$

$$\tag{8e}$$

Next, the constraints related to the information rate are reformulated by incorporating auxiliary variables $\{u_l, z_l\}$ and subsequently expressed as:

$$\frac{\left|\left(\mathbf{f}_{d,l}^H+\mathbf{f}_{r,l}^H\mathbf{\Phi}\mathbf{G}\right)\mathbf{b}_l\right|^2}{\left(\begin{array}{l}\sum\limits_{k=1,k\neq l}^{L}\left|\left(\mathbf{f}_{d,l}^H+\mathbf{f}_{r,l}^H\mathbf{\Phi}\mathbf{G}\right)\mathbf{b}_k\right|^2\\ +\mathrm{Tr}\left(\mathbf{F}_l\mathbf{V}\right)+\sigma_l^2\end{array}\right)}\geq\exp\left(\ln 2\cdot\frac{\gamma_l}{t_l}\right)-1 \tag{9}$$

Then, that is equivalent to:

$$\left|\left(\mathbf{f}_{d,l}^H+\mathbf{f}_{r,l}^H\mathbf{\Phi}\mathbf{G}\right)\mathbf{b}_l\right|^2\geq\exp\left(z_l\right)\left(\exp\left(\ln 2\cdot\gamma_l u_l\right)-1\right) \tag{10a}$$

$$\exp\left(z_l\right)\geq\sum_{k=1,k\neq l}^{L}\left|\left(\mathbf{f}_{d,l}^H+\mathbf{f}_{r,l}^H\mathbf{\Phi}\mathbf{G}\right)\mathbf{b}_k\right|^2+\mathrm{Tr}\left(\mathbf{F}_l\mathbf{V}\right)+\sigma_l^2 \tag{10b}$$

$$u_l\geq\frac{1}{t_l},u_l\geq 0 \tag{10c}$$

The problem of maximizing energy harvesting efficiency is restructured as follows:

$$\underset{\{\mathbf{b}_l,\mathbf{V},t_l,x_l,y,z_l,u_l\}}{\text{maximize}} \sum_{l=1}^{L}\frac{x_l^2}{y} \quad \text{subject to} \tag{11a}$$

$$0 \geq \frac{x_l^2}{(1-t_l)} - \sum_{k=1}^{L}\left|\left(\mathbf{f}_{d,l}^H + \mathbf{f}_{r,l}^H\mathbf{\Phi}\mathbf{G}\right)\mathbf{b}_k\right|^2 - \text{Tr}\left(\mathbf{F}_l\mathbf{V}\right), \forall l \tag{11b}$$

$$0 \geq \sum_{l=1}^{L}\|\mathbf{b}_l\|^2 + \text{Tr}\left(\mathbf{V}\right) - y \tag{11c}$$

$$0 \geq e^{z_l+\ln 2\cdot\gamma_l u_l} - e^{z_l} - \left|\left(\mathbf{f}_{d,l}^H + \mathbf{f}_{r,l}^H\mathbf{\Phi}\mathbf{G}\right)\mathbf{b}_l\right|^2, \forall l \tag{11d}$$

$$0 \geq \sum_{k=1,k\neq l}^{L}\left|\left(\mathbf{f}_{d,l}^H + \mathbf{f}_{r,l}^H\mathbf{\Phi}\mathbf{G}\right)\mathbf{b}_k\right|^2 + \text{Tr}\left(\mathbf{F}_l\mathbf{V}\right) + \sigma_l^2 - e^{z_l}, \forall l \tag{11e}$$

$$0 \geq \frac{1}{t_l} - u_l, \forall l \tag{11f}$$

$$x_l \geq 0, y \geq 0, u_l \geq 0, 1 \geq t_l \geq 0, \forall l \tag{11g}$$

$$0 \geq \sum_{l=1}^{L}\|\mathbf{b}_l\|^2 + \text{Tr}\left(\mathbf{V}\right) - P_{T,\max} \tag{11h}$$

$$\mathbf{V} \succeq 0. \tag{11i}$$

Clearly, the objective function and constraints (11b), (11d), and (11e) exhibit non-convexity. To address these complexities, we utilize the Taylor series expansion to approximate the objective function around a given fixed point $\left\{x_l^{(i)}, y^{(i)}\right\}$ as follows:

$$\frac{x_l^2}{y} \geq \frac{x_l^{(i)2}}{y^{(i)}} + \begin{bmatrix} \frac{2\,x_l^{(i)}}{y^{(i)}}\left(x_l - x_l^{(i)}\right) \\ -\frac{x_l^{(i)2}}{y^{(i)2}}\left(y - y^{(i)}\right) \end{bmatrix} = \frac{2\,x_l^{(i)}}{y^{(i)}}x_l - \frac{x_l^{(i)2}}{y^{(i)2}}y \tag{12}$$

In a similar manner, for a given fixed point $z_l^{(i)}$, the lower-bound approximation is obtained as

$$e^{z_l} \geq e^{z_l^{(i)}} + e^{z_l^{(i)}}\left(z_l - z_l^{(i)}\right) \tag{13}$$

$$\begin{aligned}\left|\left(\mathbf{f}_{d,l}^H + \mathbf{f}_{r,l}^H\mathbf{\Phi}\mathbf{G}\right)\mathbf{b}_k\right|^2 &= \mathbf{b}_k^H\mathbf{f}_l\mathbf{f}_l^H\mathbf{b}_k \\ &\geq 2\text{Re}\left\{\mathbf{b}_k^{(i)H}\mathbf{f}_l\mathbf{f}_l^H\mathbf{b}_k\right\} - \mathbf{b}_k^{(i)H}\mathbf{f}_l\mathbf{f}_l^H\mathbf{b}_k^{(i)}, \forall k,l\end{aligned} \tag{14}$$

with $\mathbf{f}_l^H = \mathbf{f}_{d,l}^H + \mathbf{f}_{r,l}^H\mathbf{\Phi}\mathbf{G}$. Slack variables $\{c_{1,l}, c_2, c_{3,l}, c_{4,l}, c_{5,l}, c_6\}$ are introduced to obtain feasible initial points for the SCA algorithm [33, 44], after which the subproblem is formulated as follows.

$$\begin{aligned}&\underset{\left\{\begin{smallmatrix}\mathbf{b}_l,\mathbf{V},t_l,x_l,y,z_l,u,\\ c_{1,l},c_2,c_{3,l},c_{4,l},c_{5,l},c_6\end{smallmatrix}\right\}}{\text{maximize}} \sum_{l=1}^{L}\left(\frac{2\,x_l^{(i)}}{y^{(i)}}x_l - \frac{x_l^{(i)2}}{y^{(i)2}}y\right) \quad \text{subject to} \\ &-\lambda\left(\sum_{l=1}^{L}\left(c_{1,l}+c_{3,l}+c_{4,l}+c_{5,l}\right) + c_2 + c_6\right)\end{aligned} \tag{15a}$$

$$0 \geq \begin{pmatrix} \frac{x_l^2}{(1-t_l)} \\ -\text{Tr}\left(\mathbf{F}_l\mathbf{V}\right) \end{pmatrix} - \sum_{k=1}^{L}\begin{pmatrix} 2\text{Re}\left\{\mathbf{b}_k^{(i)H}\mathbf{f}_l\mathbf{f}_l^H\mathbf{b}_k\right\} \\ -\mathbf{b}_k^{(i)H}\mathbf{f}_l\mathbf{f}_l^H\mathbf{b}_k^{(i)} \end{pmatrix} - c_{1,l}, \forall l \tag{15b}$$

$$0 \geq \sum_{l=1}^{L}\|\mathbf{b}_l\|^2 + \text{Tr}\left(\mathbf{V}\right) - y - c_2 \tag{15c}$$

$$0 \geq \begin{pmatrix} e^{z_l+\ln 2\cdot\gamma_l u_l} - \left(e^{z_l^{(i)}} + e^{z_l^{(i)}}\left(z_l - z_l^{(i)}\right)\right) \\ -\left(2\text{Re}\left\{\mathbf{b}_l^{(i)H}\mathbf{f}_l\mathbf{f}_l^H\mathbf{b}_l\right\} - \mathbf{b}_l^{(i)H}\mathbf{f}_l\mathbf{f}_l^H\mathbf{b}_l^{(i)}\right) \end{pmatrix} - c_{3,l}, \forall l \tag{15d}$$

$$0 \geq \begin{pmatrix} \sum_{k=1,k\neq l}^{L}\left|\left(\mathbf{f}_{d,l}^H + \mathbf{f}_{r,l}^H\mathbf{\Phi}\mathbf{G}\right)\mathbf{b}_k\right|^2 + \text{Tr}\left(\mathbf{F}_l\mathbf{V}\right) \\ +\sigma_l^2 - \left(e^{z_l^{(i)}} + e^{z_l^{(i)}}\left(z_l - z_l^{(i)}\right)\right) \end{pmatrix} - c_{4,l}, \forall l \tag{15e}$$

$$0 \geq \frac{1}{t_l} - u_l - c_{5,l}, \forall l \tag{15f}$$

$$0 \geq \sum_{l=1}^{L}\|\mathbf{b}_l\|^2 + \text{Tr}\left(\mathbf{V}\right) - P_{T,\max} - c_6 \tag{15g}$$

$$\mathbf{V} \succeq 0, x_l \geq 0, y \geq 0, u_l \geq 0, 1 \geq t_l \geq 0, \forall l \tag{15h}$$

$$c_{1,l} \geq 0, c_2 \geq 0, c_{3,l} \geq 0, c_{4,l} \geq 0, c_{5,l} \geq 0, c_6 \geq 0, \forall l. \tag{15i}$$

Then, the convex optimization subproblem (15) is effectively addressed by the CVX solver [45]. The process begins by setting the initial point as

$$\mathbf{b}_l^{(0)} = \frac{P_{T,\max}}{L\times M}[1,...,1]^T, \text{ i.e., } \left\|\mathbf{b}_l^{(0)}\right\|^2 = \frac{P_{T,\max}}{L}, \forall l. \tag{16}$$

As a result, $\sum_{l=1}^{L}\left\|\mathbf{b}_l^{(0)}\right\|^2 = P_{T,\max}$, and $z_l^{(0)} = 0$, $x_l^{(0)} = 1$, $y^{(0)} = 1$. To address the non-convex optimization problem of transceiver parameters (11), we apply the SCA method where the non-convex functions in the objective and constraints are approximated as shown in (12), (13), and (14). The SCA iteration requires an initial feasible point for the original problem (11) to ensure convergence. However, it is difficult to obtain a feasible point in problem (11). Therefore, by inserting the slack variables $\{c_{1,l}, c_2, c_{3,l}, c_{4,l}, c_{5,l}, c_6\}$ into constraints (11b) – (11g), resulting in the reformulated problem (15). We observe that any initial point $\{\mathbf{b}_l, \mathbf{V}, x_l, y, u_l, t_l\}$, can become a feasible point since appropriate values of slack variables can be chosen to satisfy the modified constraints in (11b) – (11g). Therefore, in Algorithm 1,

we can start with the initial feasible point given in (16). Ultimately, the developed iterative approach is outlined in Algorithm 1.

Algorithm 1 The developed iterative method for determining the BS beamforming vectors, energy covariance matrix, and TS factor allocations.

1: **Initialization:**
Start a feasible initial point of problem (11) as (16). Convergent accuracies ζ_1 and ζ_2. Set initial index $i = 0$. Set maximum iteration number, $T_{\max}$.
2: **Repeat**
3: Resolve the optimization problem (15) to determine the optimal solution $\left\{\mathbf{b}_l^\dagger, \mathbf{V}^\dagger, t_l^\dagger, x_l^\dagger, y^\dagger, z_l^\dagger, u^\dagger, c_{1,l}^\dagger, c_2^\dagger, c_{3,l}^\dagger, c_{4,l}^\dagger, c_{5,l}^\dagger, c_6^\dagger\right\}$ with a fixed point $\left\{\mathbf{b}_l^{(i)}, t_l^{(i)}, x_l^{(i)}, y^{(i)}, z_l^{(i)}\right\}$.
4: Assign $\mathbf{b}_l^{(i+1)} = \mathbf{b}_l^\dagger$, $t_l^{(i+1)} = t_l^\dagger$, $x_l^{(i+1)} = x_l^\dagger$, $y^{(i+1)} = y^\dagger$, $z_l^{(i+1)} = z_l^\dagger$.
5: Set $i = i + 1$
6: **Until** ($\sum_{l=1}^{L}\left(c_{1,l}^\dagger + c_{3,l}^\dagger + c_{4,l}^\dagger + c_{5,l}^\dagger\right) + c_2^\dagger + c_6^\dagger \le \zeta_1$ and $\left|\left(\sum_{l=1}^{L}\frac{x_l^{(i)2}}{y^{(i)}} - \sum_{l=1}^{L}\frac{x_l^{(i-1)2}}{y^{(i-1)}}\right) / \sum_{l=1}^{L}\frac{x_l^{(i-1)2}}{y^{(i-1)}}\right| \le \zeta_2$) or $i = T_{\max}$.
7: **Outputs:**
Optimal solution $\left\{\mathbf{b}_l^{(i)}, t_l^{(i)}, x_l^{(i)}, y^{(i)}, z_l^{(i)}, \mathbf{V}^{(i)}\right\}$, and energy harvesting efficiency $\frac{\sum_{l=1}^{L}\left[\left(1-t_l^{(i)}\right)\left(\sum_{k=1}^{L}\left\|\left(\mathbf{f}_{d,l}^H+\mathbf{f}_{r,l}^H\mathbf{\Phi}\mathbf{G}\right)\mathbf{b}_k^{(i)}\right\|^2+\mathrm{Tr}(\mathbf{F}_l\mathbf{V})\right)\right]}{\sum_{l=1}^{L}\left\|\mathbf{b}_l^{(i)}\right\|^2+\mathrm{Tr}(\mathbf{V})}$.

3.2. Design for Continuous Phase Shifts with Fixed BS and Users Parameters

Via the AO method, we will find the continuous phase shifts in problem (17) after solving the group of $\{\mathbf{b}_l, \mathbf{V}, t_l\}$ variables as follows.

$$\underset{\{\varphi_n\}}{\text{maximize}}\ 0 \quad \text{subject to} \tag{17a}$$

$$0 \ge \frac{x_l^2}{(1-t_l)} - \sum_{k=1}^{L}\left|\left(\mathbf{f}_{d,l}^H + \mathbf{f}_{r,l}^H\mathbf{\Phi}\mathbf{G}\right)\mathbf{b}_k\right|^2 - \mathrm{Tr}\left(\mathbf{F}_l\mathbf{V}\right), \forall l \tag{17b}$$

$$0 \ge e^{z_l + \ln 2\cdot\gamma_l u_l} - e^{z_l} - \left|\left(\mathbf{f}_{d,l}^H + \mathbf{f}_{r,l}^H\mathbf{\Phi}\mathbf{G}\right)\mathbf{b}_l\right|^2, \forall l \tag{17c}$$

$$0 \ge \sum_{k=1,k\ne l}^{L}\left|\left(\mathbf{f}_{d,l}^H + \mathbf{f}_{r,l}^H\mathbf{\Phi}\mathbf{G}\right)\mathbf{b}_k\right|^2 + \mathrm{Tr}\left(\mathbf{F}_l\mathbf{V}\right) + \sigma_l^2 - e^{z_l}, \forall l \tag{17d}$$

where $\mathbf{F}_l = \left(\mathbf{f}_{d,l}^H + \mathbf{f}_{r,l}^H\mathbf{\Phi}\mathbf{G}\right)^H\left(\mathbf{f}_{d,l}^H + \mathbf{f}_{r,l}^H\mathbf{\Phi}\mathbf{G}\right)$. We denote the new variable $\mathbf{q} = \left[e^{j\varphi_1}, e^{j\varphi_2}, \cdots, e^{j\varphi_N}\right]^H$, with $\left|[\mathbf{q}]_n\right| = |q_n| = 1$, $\forall n$, then derive as

$$\begin{aligned}\left|\left(\mathbf{f}_{d,l}^H + \mathbf{f}_{r,l}^H\mathbf{\Phi}\mathbf{G}\right)\mathbf{b}_k\right|^2 &= \left|\left(\mathbf{f}_{d,l}^H + \mathbf{q}^H diag\left(\mathbf{f}_{r,l}^H\right)\mathbf{G}\right)\mathbf{b}_k\right|^2 \\ &= \left|\mathbf{f}_{d,l}^H\mathbf{b}_k + \mathbf{q}^H diag\left(\mathbf{f}_{r,l}^H\right)\mathbf{G}\mathbf{b}_k\right|^2 = \left|o_{l,k} + \mathbf{q}^H\mathbf{p}_{l,k}\right|^2\end{aligned} \tag{18}$$

where $o_{l,k} = \mathbf{f}_{d,l}^H\mathbf{b}_k$ and $\mathbf{p}_{l,k} = diag\left(\mathbf{f}_{r,l}^H\right)\mathbf{G}\mathbf{b}_k$. Then,

$$\begin{aligned}\left|o_{l,k} + \mathbf{q}^H\mathbf{p}_{l,k}\right|^2 &= \left(o_{l,k} + \mathbf{q}^H\mathbf{p}_{l,k}\right)^H\left(o_{l,k} + \mathbf{q}^H\mathbf{p}_{l,k}\right) \\ &= o_{l,k}^H o_{l,k} + 2\mathrm{Re}\left\{\left(o_{l,k}^H\mathbf{p}_{l,k}\right)^H\mathbf{q}\right\} + \mathbf{q}^H\mathbf{p}_{l,k}\mathbf{p}_{l,k}^H\mathbf{q}\end{aligned} \tag{19}$$

We use equation (19) to obtain the following expression:

$$\begin{aligned}\sum_{k=1}^{L}\left|\left(\mathbf{f}_{d,l}^H + \mathbf{f}_{r,l}^H\mathbf{\Phi}\mathbf{G}\right)\mathbf{b}_k\right|^2 &= \sum_{k=1}^{L} o_{l,k}^H o_{l,k} + \\ 2\mathrm{Re}\left\{\left(\sum_{k=1}^{L} o_{l,k}^H\mathbf{p}_{l,k}\right)^H\mathbf{q}\right\} &+ \mathbf{q}^H\left(\sum_{k=1}^{L}\mathbf{p}_{l,k}\mathbf{p}_{l,k}^H\right)\mathbf{q}\end{aligned} \tag{20}$$

and approximations:

$$\mathbf{q}^H\left(\sum_{k=1}^{L}\mathbf{p}_{l,k}\mathbf{p}_{l,k}^H\right)\mathbf{q} \ge \begin{pmatrix} 2\mathrm{Re}\left\{\mathbf{q}^{(w)H}\left(\sum_{k=1}^{L}\mathbf{p}_{l,k}\mathbf{p}_{l,k}^H\right)\mathbf{q}\right\} \\ -\mathbf{q}^{(w)H}\left(\sum_{k=1}^{L}\mathbf{p}_{l,k}\mathbf{p}_{l,k}^H\right)\mathbf{q}^{(w)}\end{pmatrix} \tag{21}$$

$$\mathbf{q}^H\mathbf{p}_{l,l}\mathbf{p}_{l,l}^H\mathbf{q} \ge \begin{pmatrix} 2\mathrm{Re}\left\{\mathbf{q}^{(w)H}\mathbf{p}_{l,l}\mathbf{p}_{l,l}^H\mathbf{q}\right\} \\ -\mathbf{q}^{(w)H}\mathbf{p}_{l,l}\mathbf{p}_{l,l}^H\mathbf{q}^{(w)}\end{pmatrix}. \tag{22}$$

For the covariance matrix $\mathbf{V}$, we perform the eigendecompostion as

$$\begin{aligned}\mathbf{V} &= \sum_{m=1}^{M}\lambda_m\tilde{\mathbf{v}}_m\tilde{\mathbf{v}}_m^H = \sum_{m=1}^{M}\left(\sqrt{\lambda_m}\tilde{\mathbf{v}}_m\right)\left(\sqrt{\lambda_m}\tilde{\mathbf{v}}_m\right)^H \\ &= \sum_{m=1}^{M}\mathbf{v}_m\mathbf{v}_m^H\end{aligned} \tag{23}$$

where λ_m and are the eigenvalue and the corresponding eigenvector couples of $\mathbf{V}$, and $\mathbf{v}_m = \sqrt{\lambda_m}\tilde{\mathbf{v}}_m$, $\forall m$. Therefore,

$$\begin{aligned}\mathrm{Tr}\left(\mathbf{F}_l\mathbf{V}\right) &= \sum_{m=1}^{M}\left|\left(\mathbf{f}_{d,l}^H + \mathbf{f}_{r,l}^H\mathbf{\Phi}\mathbf{G}\right)\mathbf{v}_m\right|^2 \\ &= \sum_{k=1}^{L} v_{l,m}^H v_{l,m} + \begin{pmatrix} 2\mathrm{Re}\left\{\left(\sum_{m=1}^{M} v_{l,m}^H\widehat{\mathbf{v}}_{l,m}\right)^H\mathbf{q}\right\} \\ +\mathbf{q}^H\left(\sum_{m=1}^{M}\widehat{\mathbf{v}}_{l,m}\widehat{\mathbf{v}}_{l,m}^H\right)\mathbf{q}\end{pmatrix}\end{aligned} \tag{24}$$

where $v_{l,m} = \mathbf{f}_{d,l}^H\mathbf{v}_m$ and $\widehat{\mathbf{v}}_{l,m} = diag\left(\mathbf{f}_{r,l}^H\right)\mathbf{G}\mathbf{v}_m, \forall m$. Then, the lower-bound approximation of the convex

function is expressed as

$$\mathbf{q}^H\left(\sum_{m=1}^{M}\widehat{\mathbf{v}}_{l,m}\widehat{\mathbf{v}}_{l,m}^H\right)\mathbf{q} \geq \begin{pmatrix} 2\mathrm{Re}\left\{\mathbf{q}^{(w)H}\left(\sum_{m=1}^{M}\widehat{\mathbf{v}}_{l,m}\widehat{\mathbf{v}}_{l,m}^H\right)\mathbf{q}\right\} \\ -\mathbf{q}^{(w)H}\left(\sum_{m=1}^{M}\widehat{\mathbf{v}}_{l,m}\widehat{\mathbf{v}}_{l,m}^H\right)\mathbf{q}^{(w)} \end{pmatrix} \tag{25}$$

with the fixed point $\mathbf{q}^{(w)}$. To analyse $\left|[\mathbf{q}]_n\right| = |q_n| = 1,\ \forall n$, we transform it into the equivalent formula as follows

$$|q_n|^2 = 1 \Leftrightarrow \begin{cases} |q_n|^2 \geq 1 \\ 1 \geq |q_n|^2 \end{cases} \tag{26}$$

We then approximate the convex function $|q_n|^2$ by

$$|q_n|^2 \geq 2\mathrm{Re}\left\{q_n^{(w)H} q_n\right\} - \left|q_n^{(w)H}\right|^2,\ \forall n. \tag{27}$$

Algorithm 2 The final AO-based method for the EH efficiency maximization.

1: **Initialization:** Start initial shift-phases $\left\{\varphi_n^{(0)}\right\}$, max. iteration number K_3, initial number $\kappa = 0$, and relative accuracy ζ_3.
2: **Repeat**
% *Applying AO method*
3: With fixed $\left\{\varphi_n^{(\kappa)}\right\}$, performing Algorithm 1 to achieve $\left\{\mathbf{b}_l^{(\kappa)}, \mathbf{V}^{(\kappa)}, t_l^{(\kappa)}\right\}$ by solving subproblem (11) via SCA and FPP methods.
4: With fixed $\left\{\mathbf{b}_l^{(\kappa)}, \mathbf{V}^{(\kappa)}, t_l^{(\kappa)}\right\}$, obtain $\left\{\varphi_n^{(\kappa+1)}\right\}$ by solving subproblem (17) via SCA and FPP methods.
5: Assign $\kappa = \kappa + 1$.
6: **Until** $\frac{\left|f_{EHE}\left(\mathbf{b}_l^{(\kappa)},\mathbf{V}^{(\kappa)},t_l^{(\kappa)},\varphi_n^{(\kappa)}\right) - f_{EHE}\left(\mathbf{b}_l^{(\kappa-1)},\mathbf{V}^{(\kappa-1)},t_l^{(\kappa-1)},\varphi_n^{(\kappa-1)}\right)\right|}{f_{EHE}\left(\mathbf{b}_l^{(\kappa-1)},\mathbf{V}^{(\kappa-1)},t_l^{(\kappa-1)},\varphi_n^{(\kappa-1)}\right)} \leq \zeta_3$ or $\kappa = K_3$.
7: **Outputs:**
Optimal solution $\left\{\mathbf{b}_l^*, \mathbf{V}^*, t_l^*, \varphi_n^*\right\} \leftarrow \left\{\mathbf{b}_l^{(\kappa)}, \mathbf{V}^{(\kappa)}, t_l^{(\kappa)}, \varphi_n^{(\kappa)}\right\}$ and optimal value $f_{EHE}^* \leftarrow f_{EHE}\left(\mathbf{b}_l^{(\kappa)}, \mathbf{V}^{(\kappa)}, t_l^{(\kappa)}, \varphi_n^{(\kappa)}\right)$.

Since the SCA algorithm requires a feasible starting point for iterative convergence, we introduce a set of nonnegative variables $\{\theta_{1,l}, \theta_{2,l}, \theta_{3,l}, \phi_{1,n}, \phi_{2,n}\}$, $l \in \{1, \cdots, L\}$ and $n \in \{1, \cdots, N\}$, which are incorporating into the inequality constraints and penalized in the objective function using the FPP method. Thus, the tractable convex subproblem as follows:

$$\underset{\substack{\{\mathbf{q},\theta_{1,l},\theta_{2,l},\\ \theta_{3,l},\phi_{1,n},\phi_{2,n}\}}}{\text{minimize}} \begin{pmatrix} \sum_{l=1}^{L}(\theta_{1,l}+\theta_{2,l}+\theta_{3,l}) \\ +\sum_{n=1}^{N}(\phi_{1,n}+\phi_{2,n}) \end{pmatrix} \quad \text{s.t.} \tag{28a}$$

$$0 \geq \frac{x_l^2}{(1-t_l)} - \begin{pmatrix} \sum_{k=1}^{L} o_{l,k}^H o_{l,k} + 2\mathrm{Re}\left\{\left(\sum_{k=1}^{L} o_{l,k}^H \mathbf{p}_{l,k}\right)^H \mathbf{q}\right\} \\ +\begin{pmatrix} 2\mathrm{Re}\left\{\mathbf{q}^{(w)H}\left(\sum_{k=1}^{L}\mathbf{p}_{l,k}\mathbf{p}_{l,k}^H\right)\mathbf{q}\right\} \\ -\mathbf{q}^{(w)H}\left(\sum_{k=1}^{L}\mathbf{p}_{l,k}\mathbf{p}_{l,k}^H\right)\mathbf{q}^{(w)} \end{pmatrix} \end{pmatrix} - \begin{pmatrix} \sum_{k=1}^{L} v_{l,m}^H v_{l,m} + 2\mathrm{Re}\left\{\left(\sum_{m=1}^{M} v_{l,m}^H \widehat{\mathbf{v}}_{l,m}\right)^H \mathbf{q}\right\} \\ +\begin{pmatrix} 2\mathrm{Re}\left\{\mathbf{q}^{(w)H}\left(\sum_{m=1}^{M}\widehat{\mathbf{v}}_{l,m}\widehat{\mathbf{v}}_{l,m}^H\right)\mathbf{q}\right\} \\ -\mathbf{q}^{(w)H}\left(\sum_{m=1}^{M}\widehat{\mathbf{v}}_{l,m}\widehat{\mathbf{v}}_{l,m}^H\right)\mathbf{q}^{(w)} \end{pmatrix} \end{pmatrix} - \theta_{1,l}, \forall l \tag{28b}$$

$$0 \geq e^{z_l + \ln 2 \cdot \gamma_l u_l} - e^{z_l} - \begin{pmatrix} 2\mathrm{Re}\left\{\mathbf{q}^{(w)H}\mathbf{p}_{l,l}\mathbf{p}_{l,l}^H\mathbf{q}\right\} \\ -\mathbf{q}^{(w)H}\mathbf{p}_{l,l}\mathbf{p}_{l,l}^H\mathbf{q}^{(w)} \end{pmatrix} - \theta_{2,l}, \forall l \tag{28c}$$

$$0 \geq \begin{pmatrix} \sum_{k=1,k\neq l}^{L} o_{l,k}^H o_{l,k} + 2\mathrm{Re}\left\{\left(\sum_{k=1,k\neq l}^{L} o_{l,k}^H \mathbf{p}_{l,k}\right)^H \mathbf{q}\right\} \\ +\mathbf{q}^H\left(\sum_{k=1,k\neq l}^{L}\mathbf{p}_{l,k}\mathbf{p}_{l,k}^H\right)\mathbf{q} \end{pmatrix} + \begin{pmatrix} \sum_{k=1}^{L} v_{l,m}^H v_{l,m} + 2\mathrm{Re}\left\{\left(\sum_{m=1}^{M} v_{l,m}^H \widehat{\mathbf{v}}_{l,m}\right)^H \mathbf{q}\right\} \\ +\mathbf{q}^H\left(\sum_{m=1}^{M}\widehat{\mathbf{v}}_{l,m}\widehat{\mathbf{v}}_{l,m}^H\right)\mathbf{q} \end{pmatrix} + \sigma_l^2 - e^{z_l} - \theta_{3,l}, \forall l \tag{28d}$$

$$\left(2\mathrm{Re}\left\{q_n^{(w)H} q_n\right\} - \left|q_n^{(w)H}\right|^2\right) \geq 1 - \phi_{1,n}, \forall n \tag{28e}$$

$$1 \geq |q_n|^2 - \phi_{2,n}, \forall n \tag{28f}$$

$$\theta_{1,l} \geq 0, \theta_{2,l} \geq 0, \theta_{3,l} \geq 0, \phi_{1,n} \geq 0, \phi_{1,n} \geq 0, \forall l, n. \tag{28g}$$

After solving this convex subproblem with CVX, $\mathbf{q}^{(w)}$ is assigned by the optimal solution $\mathbf{q}^\dagger$ for the next iteration. The SCA iteration is convergent when the sum of auxiliary variables $\{\theta_{1,l}, \theta_{2,l}, \theta_{3,l}, \phi_{1,n}, \phi_{2,n}\}$ falls below the threshold ζ_3. The procedure for solving the problem follows a similar approach to Algorithm 1. Using alternating manner of the AO approach, the final AO-based method is presented to achieve the near-optimal values of BS vector, energy covariance matrix, TS factors, and continuous phase-shifts for the EH efficiency maximization as follows.

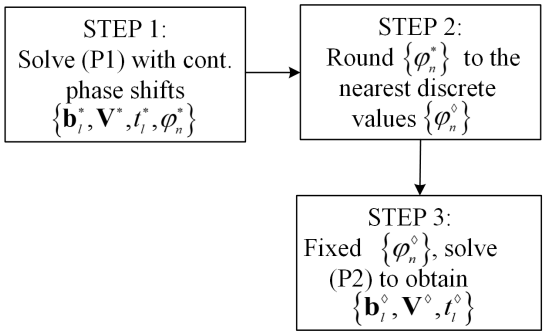

Figure 2. Diagram of proposed solution for discrete phase shifts.

The computational complexity of solving problem (15) mainly depends on $\left(2M^2 + 2LM + 3L + 1\right)$ real variables and $(5L + 1)$ conic constraints, thus it is computed as $\mathcal{O}\left(K_1\sqrt{(5L+1)}\left(2M^2 + 2LM + 3L + 1\right)^3\right)$ with iteration number K_1 in Algorithm 1 and the big-O notation $\mathcal{O}(\cdot)$ [46]. Similarly, the complexity of solving problem (17) is $\mathcal{O}\left(K_2\sqrt{(3L+2N)}(4N+3L)^3\right)$ with $(4N + 3L)$ real variables and $(3L + 2N)$ conic constraints and iteration number K_2. Therefore, the overall complexity of solving problem (7) is $\mathcal{O}\left(K_3\left(\begin{array}{l} K_2\sqrt{(5L+1)}\left(2M^2 + 2LM + 3L + 1\right)^3 \\ +K_2\sqrt{(3L+2N)}(4N+3L)^3 \end{array}\right)\right)$ with iteration number K_3 in Algorithm 2.

3.3. Scheme of IRS Discrete Phase Shifts

In a practical IRS circuit, the phase-shift angles are restricted to a finite set of values within the range of $\{\varphi_n\}$. Specifically, denotes the bit resolution for uniform quantization within $[0, 2\pi)$. Consequently, all possible phase-shift values are confined to a predefined discrete set $\left\{0, \frac{2\pi}{2^D}, \cdots, \frac{2\pi\times(2^D-1)}{2^D}\right\}$. In this case, the continuous phase shifts at IRS are optimized with Subsections 3.2 and 3.3, then the optimal phase shifts $\{\varphi_n^*\}$ are rounded the nearest discrete values in the phase-shift set. To satisfy the constraints of problem (7), we resolve problem (11) with the new discrete results of phase shifts to obtain the suboptimal BS beamforming vector, energy covariance matrix, and TS factors. Then, Fig. 2 expresses the diagram of proposed solution for the discrete phase-shift case.

4. Simulation Evaluations

Numerical simulations are conducted to validate the efficiency of the proposed algorithm. The network topology is configured as follows: The BS and the IRS are positioned at coordinates (0, 0) and (3, 2.5) in meters, respectively. Furthermore, L receivers equipped with TS architectures are uniformly distributed on a circular region centered at (5, 0) with a radius of 0.5

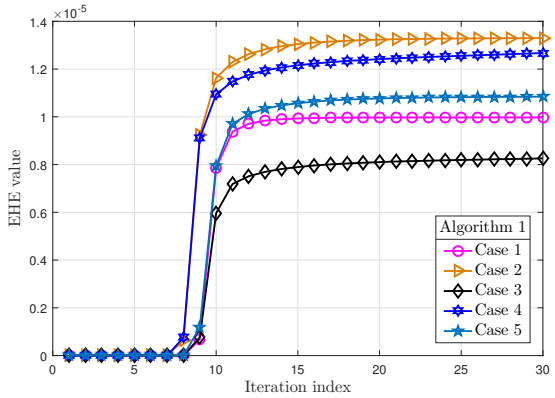

Figure 3. The numerical behavior of proposed Algorithm 1.

meters. The large-scale path loss for each communication link is modeled as $PL = 10^{-3}d^{-\alpha}$, where α denotes the path loss exponent. The attenuation parameters for the BS-to-IRS, IRS-to-User, and BS-to-User connections are specified as $\alpha_{\text{BI}} = 2.2$, $\alpha_{\text{IU}} = 2.2$, and $\alpha_{\text{BU}} = 3.6$, respectively [47]. Additionally, small-scale fading in all channels follows the Rician fading model, with the Rician factor set to 3. Accordingly, the channel model from the BS to the IRS can be expressed as:

$$\mathbf{G} = \sqrt{10^{-3}d_{\text{BI}}^{-\alpha}}\left(\sqrt{\frac{\beta}{1+\beta}}\mathbf{G}^{\text{LoS}} + \sqrt{\frac{1}{1+\beta}}\mathbf{G}^{\text{NLoS}}\right) \quad (29)$$

where d_{BI} is the distance from BS to IRS. Moreover, $\mathbf{G}^{\text{LoS}}$ and $\mathbf{G}^{\text{NLoS}}$ represent the deterministic light-of-sight (LoS) and non-LoS components, respectively. The LoS part is derived by the product of the steering vectors of the BS and IRS where all elements are assumed to be unity for simplicity. The non-LoS part is modeled using Rayleigh fading with identical independent distribution (i.i.d.). The AP-user and IRS-user links are generated using a similar formulation. Furthermore, the power of the additive noise at the receiving nodes is $\sigma_l^2 = -60$ dBm,$\forall l$. The quantization resolution is determined via simulation cases and the initial phase shifts are randomly initialized. The performance of the proposed method is assessed by analyzing its convergence across multiple random channel realizations and by evaluating the impact of various system parameters.

4.1. Convergent Behavior of Proposed Iterative Algorithms

The convergent behaviors are illustrated to evaluate the effectiveness o f p roposed A lgorithms 1 a nd 2 under the several channel trials in Figs. 3 and 4. In Fig. 3, the initial phase shifts for different c hannel t rials are assigned randomly with the penalty factor $\lambda = 10^3$. The slack variables $\{c_{1,l}, c_2, c_{3,l}, c_{4,l}, c_{5,l}, c_6\}$ allow the initial

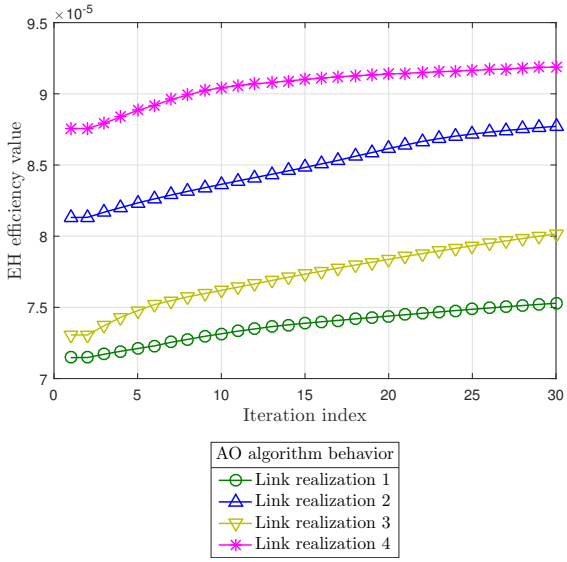

Figure 4. The numerical expression of proposed Algorithm 2.

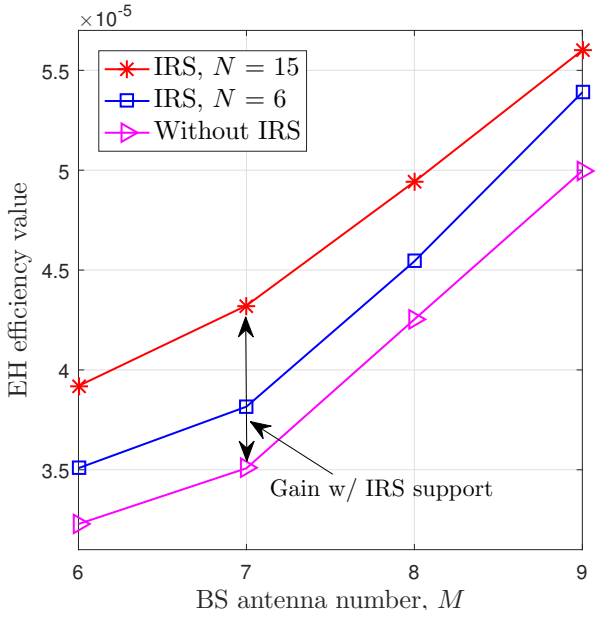

Figure 5. EH efficiency results via BS antenna number.

point of the SCA iteration (16) to be feasible and then converge to zero by penalty technique. We observe the objective value converges fast after about 20 iterations. In Fig. 4, it can be seen that the objective value increases after each iteration and achieves the convergence in approximately 30 iterations. In the network scenarios, the suboptimal value of EH efficiency is about 10^{-5} and the initial phase shifts are randomly selected from $[0, 2\pi)$.

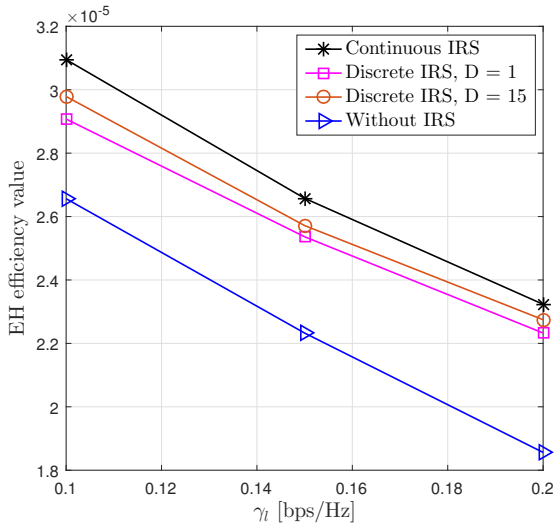

Figure 6. EH efficiency results via data rate threshold.

4.2. Effect of BS Antenna Number

The maximum EH efficiency as a function of the number of BS antennas is shown in Fig. 5 with the number of IRS elements set to $N = 6, 15$, the data rate threshold $\gamma_l = 0.1$ bps/Hz, and the transmission power budget $P_{T,\max} = 60$ dBW. We observe that when the number of BS antennas increases from 6 to 9, the value of EH efficiency also rises from 3.25×10^{-5} to 5.19×10^{-5} for $N = 15$. In comparison to the case without IRS support, at $M = 7$, the gain of EH efficiency with $N = 15$ reaches 23.08 %. Moreover, the higher EH efficiency is obtained with the increase in the number of IRS components.

4.3. Effect of Data Rate Threshold

In Fig. 6, the effect of data rate threshold on EH efficiency results is presented with the BS antenna number, $M = 4$, and the IRS component number, $N = 8$, and the transmission power $P_{T,\max} = 30$ dBW. As shown in Fig. 6, the SWIPT system with the support of continuous phase-shift IRS is able to enhance the EH efficiency value compared with both the case without IRS and the case with discrete phase-shift IRS. Moreover, an increase in the data-rate threshold requires more energy information decoding, which consequently reduces EH efficiency.

4.4. Effect of IRS Component Number

In Fig. 7 with bar plots, we illustrate EH efficiency versus the number of IRS reflectors under network settings $M = 10$ and $\gamma_l = 0.1$ bps/Hz, comparing the IRS-assisted scheme with the scheme without IRS. It is observed that as the number of IRS elements increases, the performance gap between the IRS assistance scheme

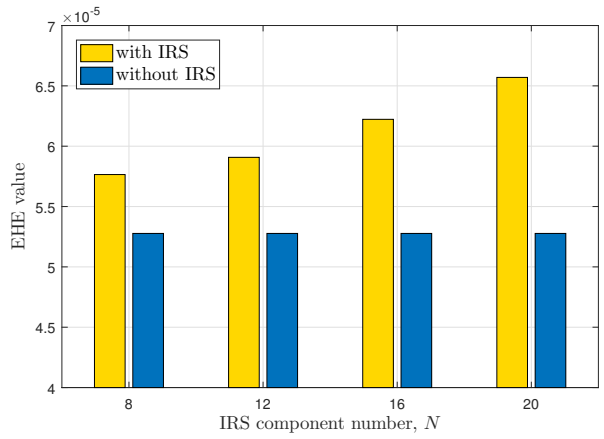

Figure 7. EH efficiency results via IRS component number.

and the scheme without IRS widens. This improvement results from the higher reflection accuracy when N increases.

5. Conclusion

In this work, we studied an IRS-assisted SWIPT network with TS receivers, unicast transmission mode, and both continuous and discrete IRS phase shifts of IRS. The proposed solution aims to maximize the EH efficiency while satisfying constraints on user data rates, transmission power budget of the BS, TS factor intervals, and the unit-modulus of IRS reflection matrix. Specifically, the AO technique is employed to decouple transceiver parameters and IRS phase adjustments, while the SCA approach is utilized to tackle the highly non-convex optimization challenges related to EH efficiency, information rate limitations, and phase-shift constraints. Numerical results show that the IRS support can enhance EH efficiency compared to the case without IRS in the considered SWIPT network. Furthermore, the proposed algorithm exhibits strong convergence behavior, and the EH efficiency improves as the number of BS antennas and IRS elements increases.

5.1. Acknowledgements

This research is funded by University of Education, Hue University under grant number NCTB-T.24-TN.103.02. The authors also acknowledge the partial support of Hue University under the Core Research Program, Grant No. NCTB.DHH.2025.17.

References

[1] Jiang, W., Han, B., Habibi, M.A. and Schotten, H.D. (2021) The road towards 6g: A comprehensive survey. *IEEE Open Journal of the Communications Society* **2**: 334–366. doi:10.1109/OJCOMS.2021.3057679.

[2] Nguyen, D.C., Ding, M., Pathirana, P.N., Seneviratne, A., Li, J., Niyato, D., Dobre, O. *et al.* (2021) 6g internet of things: A comprehensive survey. *IEEE Internet of Things Journal* **9**(1): 359–383. doi:10.1109/JIOT.2021.3103320.

[3] De Alwis, C., Kalla, A., Pham, Q.V., Kumar, P., Dev, K., Hwang, W.J. and Liyanage, M. (2021) Survey on 6g frontiers: Trends, applications, requirements, technologies and future research. *IEEE Open Journal of the Communications Society* **2**: 836–886. doi:10.1109/OJCOMS.2021.3071496.

[4] Xu, J., Liu, L. and Zhang, R. (2014) Multiuser miso beamforming for simultaneous wireless information and power transfer. *IEEE Transactions on Signal Processing* **62**(18): 4798–4810. doi:10.1109/TSP.2014.2340817.

[5] Ashraf, N., Sheikh, S.A., Liaqat, M. and Khan, S.A. (2025) Performance analysis of swipt-assisted cooperative noma network with non-linear eh, interference and imperfect sic. *IEEE Access* doi:10.1109/ACCESS.2025.3563111.

[6] Zhao, N., Zhang, S., Yu, F.R., Chen, Y., Nallanathan, A. and Leung, V.C. (2017) Exploiting interference for energy harvesting: A survey, research issues, and challenges. *IEEE Access* **5**: 10403–10421. doi:10.1109/ACCESS.2017.2705638.

[7] Perera, T.D.P., Jayakody, D.N.K., Sharma, S.K., Chatzinotas, S. and Li, J. (2017) Simultaneous wireless information and power transfer (swipt): Recent advances and future challenges. *IEEE Communications Surveys & Tutorials* **20**(1): 264–302. doi:10.1109/COMST.2017.2783901.

[8] Krikidis, I., Timotheou, S., Nikolaou, S., Zheng, G., Ng, D.W.K. and Schober, R. (2014) Simultaneous wireless information and power transfer in modern communication systems. *IEEE Communications Magazine* **52**(11): 104–110. doi:10.1109/MCOM.2014.6957150.

[9] Clerckx, B., Zhang, R., Schober, R., Ng, D.W.K., Kim, D.I. and Poor, H.V. (2018) Fundamentals of wireless information and power transfer: From rf energy harvester models to signal and system designs. *IEEE Journal on Selected Areas in Communications* **37**(1): 4–33. doi:10.1109/JSAC.2018.2872615.

[10] Psomas, C., Ntougias, K., Shanin, N., Xu, D., Mayer, K., Tran, N.M., Cottatellucci, L. *et al.* (2024) Wireless information and energy transfer in the era of 6g communications. *Proceedings of the IEEE* doi:10.1109/JPROC.2024.3395178.

[11] Lee, H., Lee, K.J., Kim, H. and Lee, I. (2018) Joint transceiver optimization for miso swipt systems with time switching. *IEEE Transactions on Wireless Communications* **17**(5): 3298–3312. doi:10.1109/TWC.2018.2809734.

[12] Tang, J., Luo, J., Liu, M., So, D.K., Alsusa, E., Chen, G., Wong, K.K. *et al.* (2019) Energy efficiency optimization for noma with swipt. *IEEE Journal of Selected Topics in Signal Processing* **13**(3): 452–466. doi:10.1109/JSTSP.2019.2898114.

[13] Jiang, R., Xiong, K., Fan, P., Zhang, Y. and Zhong, Z. (2019) Power minimization in swipt networks with coexisting power-splitting and time-switching users under nonlinear eh model. *IEEE Internet of Things Journal* **6**(5): 8853–8869. doi:10.1109/JIOT.2019.2923977.

[14] Goktas, M.B., Dursun, Y. and Ding, Z. (2023) Irs and swipt-assisted full-duplex noma for 6g ummtc. *IEEE Transactions on Green Communications and Networking* **7**(4): 1957–1970. doi:10.1109/TGCN.2023.3289505.

[15] Wu, Q., Guan, X. and Zhang, R. (2021) Intelligent reflecting surface-aided wireless energy and information transmission: An overview. *Proceedings of the IEEE* **110**(1): 150–170. doi:10.1109/JPROC.2021.3121790.

[16] Han, H., Zhao, J., Zhai, W., Xiong, Z., Niyato, D., Di Renzo, M., Pham, Q.V. *et al.* (2021) Reconfigurable intelligent surface aided power control for physical-layer broadcasting. *IEEE Transactions on Communications* **69**(11): 7821–7836. doi:doi=10.1109/TCOMM.2021.3104871.

[17] Basar, E., Alexandropoulos, G.C., Liu, Y., Wu, Q., Jin, S., Yuen, C., Dobre, O.A. *et al.* (2024) Reconfigurable intelligent surfaces for 6g: Emerging hardware architectures, applications, and open challenges. *IEEE Vehicular Technology Magazine* doi:10.1109/MVT.2024.3415570.

[18] Wu, Q. and Zhang, R. (2019) Weighted sum power maximization for intelligent reflecting surface aided swipt. *IEEE Wireless Communications Letters* **9**(5): 586–590. doi:10.1109/LWC.2019.2961656.

[19] Sadia, H., Hassan, A.K., Abbas, Z.H., Abbas, G., Baker, T. and Saeed, N. (2025) Maximizing energy efficiency in irs-assisted phase cooperative ps-swipt based self-sustainable iot network. *IEEE Open Journal of the Communications Society* **6**: 4311–4327. doi:10.1109/OJCOMS.2025.3570094.

[20] Wei, Y., Peng, Z., Tang, J., Zhang, X., Wong, K.K. and Chambers, J. (2024) Max-min fair beamforming design for a ris-assisted system with swipt. *IEEE Transactions on Vehicular Technology* **73**(8): 12148–12153. doi:10.1109/TVT.2024.3371539.

[21] Zhu, G., Mu, X., Guo, L., Huang, A. and Xu, S. (2024) Robust resource allocation for star-ris assisted swipt systems. *IEEE Transactions on Wireless Communications* **23**(6): 5616–5631. doi:10.1109/TWC.2023.3327502.

[22] Amiri, M., Vaezpour, E., Javadi, S., Mili, M.R., Bennis, M. and Jorswieck, E. (2025) Resource allocation in star-ris-aided swipt with rsma via meta-learning. *IEEE Open Journal of the Communications Society* doi:10.1109/OJCOMS.2025.3556484.

[23] Li, Y., Wang, J., Zou, Y., Xie, W. and Liu, Y. (2024) Weighted sum power maximization for star-ris assisted swipt systems. *IEEE Transactions on Wireless Communications* **23**(12): 18394–18408. doi:10.1109/TWC.2024.3467160.

[24] Xie, W., Qin, L., Wang, J., Wu, W., Li, X., Xu, H. and Yang, L. (2025) Simultaneous wireless information and power transfer for star-ris-assisted aav networks. *IEEE Internet of Things Journal* **12**(12): 19915–19928. doi:10.1109/JIOT.2025.3542883.

[25] Liu, J., Xiong, K., Lu, Y., Ng, D.W.K., Zhong, Z. and Han, Z. (2020) Energy efficiency in secure irs-aided swipt. *IEEE Wireless Communications Letters* **9**(11): 1884–1888. doi:10.1109/LWC.2020.3006837.

[26] Wang, T., Fang, F. and Ding, Z. (2022) An sca and relaxation based energy efficiency optimization for multi-user ris-assisted noma networks. *IEEE Transactions on Vehicular Technology* **71**(6): 6843–6847. doi:10.1109/TVT.2022.3162197.

[27] Yang, Z. and Zhang, Y. (2021) Beamforming optimization for ris-aided swipt in cell-free mimo networks. *China communications* **18**(9): 175–191. doi:10.23919/JCC.2021.09.014.

[28] Li, Z., Chen, W., Wu, Q., Wang, K. and Li, J. (2021) Joint beamforming design and power splitting optimization in irs-assisted swipt noma networks. *IEEE Transactions on Wireless Communications* **21**(3): 2019–2033. doi:10.1109/TWC.2021.3108901.

[29] Tuan, P.V. and Son, P.N. (2022) Intelligent reflecting surface assisted transceiver design optimization in non-linear swipt network with heterogeneous users. *Wireless Networks* **28**(5): 1889–1908. doi:https://doi.org/10.1007/s11276-022-02938-6.

[30] Zargari, S., Hakimi, A., Tellambura, C. and Herath, S. (2022) Multiuser miso ps-swipt systems: Active or passive ris? *IEEE Wireless Communications Letters* **11**(9): 1920–1924.

[31] Yu, X., Shen, J.C., Zhang, J. and Letaief, K.B. (2016) Alternating minimization algorithms for hybrid precoding in millimeter wave mimo systems. *IEEE Journal of Selected Topics in Signal Processing* **10**(3): 485–500. doi:10.1109/JSTSP.2016.2523903.

[32] Marks, B.R. and Wright, G.P. (1978) A general inner approximation algorithm for nonconvex mathematical programs. *Operations research* **26**(4): 681–683. doi:https://doi.org/10.1287/opre.26.4.681.

[33] Gautam, S., Lagunas, E., Chatzinotas, S. and Ottersten, B. (2021) Feasible point pursuit and successive convex approximation for transmit power minimization in swipt-multigroup multicasting systems. *IEEE Transactions on Green Communications and Networking* **5**(2): 884–894. doi:10.1109/TGCN.2021.3050736.

[34] Tuan, P.V., Nguyen-Duy-Nhat, V., Le, M.T., Nguyen, H.V., Quan, V.A.N., Son, P.N. and Koo, I. (2024) Enhancing energy harvesting efficiency for irs-aided ts-swipt network with practical phase shifts. In *International Conference on Industrial Networks and Intelligent Systems* (Springer): 155–165. doi:https://doi.org/10.1007/978-3-031-67357-3_11.

[35] Zheng, B., You, C., Mei, W. and Zhang, R. (2022) A survey on channel estimation and practical passive beamforming design for intelligent reflecting surface aided wireless communications. *IEEE Communications Surveys & Tutorials* **24**(2): 1035–1071. doi:10.1109/COMST.2022.3155305.

[36] Wang, R., Wang, Z., Liu, L., Zhang, S. and Jin, S. (2024) Reducing channel estimation and feedback overhead in irs-aided downlink system: A quantize-then-estimate approach. *IEEE Transactions on Wireless Communications* doi:10.1016/j.icte.2023.06.004.

[37] Kwon, D. and Kim, D.K. (2024) Channel estimation overhead reduction scheme and its impact in irs-assisted systems. *ICT Express* **10**(1): 58–64. doi:10.1016/j.icte.2023.06.004.

[38] Hu, S., Wei, Z., Cai, Y., Liu, C., Ng, D.W.K. and Yuan, J. (2021) Robust and secure sum-rate maximization for multiuser miso downlink systems with self-sustainable irs. *IEEE Transactions on Communications* **69**(10): 7032–7049. doi:10.1109/TCOMM.2021.3097140.

[39] Han, Y., Tang, W., Jin, S., Wen, C.K. and Ma, X. (2019) Large intelligent surface-assisted wireless communication exploiting statistical csi. *IEEE transactions on vehicular technology* **68**(8): 8238–8242. doi:10.1109/TVT.2019.2923997.

[40] Haochen, L., Zhiwen, P., Bin, W., Nan, L. and Xiaohu, Y. (2025) Statistical csi based beamforming for reconfigurable intelligent surface aided miso systems with channel correlation. *China Communications* **22**(5): 14–27. doi:10.23919/JCC.ja.2022-0713.

[41] Zhou, G., Pan, C., Ren, H., Wang, K. and Nallanathan, A. (2020) A framework of robust transmission design for irs-aided miso communications with imperfect cascaded channels. *IEEE Transactions on Signal Processing* **68**: 5092–5106. doi:10.1109/TSP.2020.3019666.

[42] Pan, C., Zhou, G., Zhi, K., Hong, S., Wu, T., Pan, Y., Ren, H. *et al.* (2022) An overview of signal processing techniques for ris/irs-aided wireless systems. *IEEE Journal of Selected Topics in Signal Processing* **16**(5): 883–917. doi:10.1109/JSTSP.2022.3195671.

[43] Grant, M. and Boyd, S. (2020), Cvx: Matlab software for disciplined convex programming, version 2.2. URL https://web.cvxr.com/cvx/cvx-w64.zip.

[44] Razaviyayn, M. (2014) *Successive convex approximation: Analysis and applications*. Ph.D. thesis, University of Minnesota. URL https://conservancy.umn.edu/server/api/core/bitstreams/88697b6c-6385-4795-9a55-cb31ec861232/content.

[45] Boyd, S. and Vandenberghe, L. (2004) *Convex optimization* (Cambridge university press). URL https://xiesaining.wordpress.com/wp-content/uploads/2012/09/mlss2011_vandenberghe_convex.pdf.

[46] Ben-Tal, A. and Nemirovski, A. (2001) *Lectures on modern convex optimization: analysis, algorithms, and engineering applications* (SIAM). URL https://www2.isye.gatech.edu/~nemirovs/lmco_run_prf.pdf.

[47] Wu, Q. and Zhang, R. (2019) Intelligent reflecting surface enhanced wireless network via joint active and passive beamforming. *IEEE transactions on wireless communications* **18**(11): 5394–5409. doi:10.1109/TWC.2019.2936025.